ADVANCED MATERIALS
www.advmat.de

Ultrafast Photoinduced Multimode Antiferromagnetic Spin Dynamics in Exchange-Coupled Fe/$RFeO_3$ (R = Er or Dy) Heterostructures

*Jin Tang, Yajiao Ke, Wei He, Xiangqun Zhang, Wei Zhang, Na Li, Yongsheng Zhang, Yan Li, and Zhaohua Cheng**

Antiferromagnetic spin dynamics is important for both fundamental and applied antiferromagnetic spintronic devices; however, it is rarely explored by external fields because of the strong exchange interaction in antiferromagnetic materials. Here, the photoinduced excitation of ultrafast antiferromagnetic spin dynamics is achieved by capping antiferromagnetic $RFeO_3$ (R = Er or Dy) with an exchange-coupled ferromagnetic Fe film. Compared with antiferromagnetic spin dynamics of bare $RFeO_3$ orthoferrite single crystals, which can be triggered effectively by ultrafast laser heating just below the phase transition temperature, the ultrafast photoinduced multimode antiferromagnetic spin dynamic modes, for exchange-coupled Fe/$RFeO_3$ heterostructures, including quasiferromagnetic resonance, impurity, coherent phonon, and quasiantiferromagnetic modes, are observed in a temperature range of 10–300 K. These experimental results not only offer an effective means to trigger ultrafast antiferromagnetic spin dynamics of rare-earth orthoferrites, but also shed light on the ultrafast manipulation of antiferromagnetic magnetization in Fe/$RFeO_3$ heterostructures.

In contrast to ferromagnetic (FM) materials, antiferromagnetic (AFM) materials usually are assumed to be invisible to common magnetic probes and insensitive to disturbing fields because of their zero macroscopic magnetization and strong AFM exchange interaction. AFM materials, however, also have some unique magnetic properties, including ultrahigh resonant frequency (typically in the terahertz [THz] range). Therefore, AFM spintronics, which aims to make AFM materials useful for high-frequency spintronic devices, are now attracting significant attention.[1] One of the most fascinating research fields for AFM materials is ultrafast spin dynamics with frequencies up to the terahertz range.

Because of their particular spin structures and abundant phase transitions, AFM spin dynamics of $RFeO_3$ (R denotes rare earth elements) first is triggered by laser heating in the vicinity of the spin reorientation transition temperature region.[2–4] The inverse Faraday effect,[3–6] inertia-driven switching,[7] optical modification of exchange interactions,[8,9] THz pulses, and optically driven phonons by mid-infrared pulse have effectively excited the AFM spin dynamics.[10–12] The use of common all-optical pump-probe techniques, however, pose two limitations to investigating the AFM spin dynamics of $RFeO_3$. First, the spin dynamics of $RFeO_3$ cannot be probed in a wide temperature range. For example, the spin dynamics of $RFeO_3$ mostly are excited by an ultrafast laser heating effect just below the spin-reorientation transition temperature.[2–4] In the case of $TmFeO_3$ and $ErFeO_3$ (EFO),[3,4] by using a circularly polarized laser, the spin precession can be excited only by the thermal and nonthermal (inverse Faraday effect) mechanisms below or around the spin-reorientation transition temperature region. Moreover, the amplitude of the dynamic signal excited by a circularly polarized laser exhibits an exponential decay trend as the temperature increases for $DyFeO_3$ (DFO).[5] Second, the modes obtained by the all-optical method are limited. There are quasiferromagnetic resonance (Q-FM),[2–4] quasiantiferromagnetic resonance (Q-AFM),[5] impurity, and phonon modes in $RFeO_3$.[10–12] Using the all-optical method, however, the impurity and phonon modes never have been probed, whereas the Q-AFM mode has been reported only in DFO. Therefore, a method to improve the efficiency of multimode AFM spin dynamics triggered by an ultrafast laser urgently needs to be developed.

Because the exchange interaction of neighboring spins is strongest among the magnetic interactions, optical modification of an interfacial exchange coupling has been proved to be an effective means to control the spin dynamics of FM coupled with an AFM.[13–17] Furthermore, optical modification of the interfacial exchange interaction is an effective technique to trigger AFM spin dynamics. Although laser-induced

Dr. J. Tang, Dr. Y. Ke, Dr. W. He, X. Zhang, W. Zhang, N. Li, Dr. Y. Zhang, Y. Li, Prof. Z. Cheng
State Key Laboratory of Magnetism and Beijing National Laboratory for Condensed Matter Physics
Institute of Physics
Chinese Academy of Sciences
Beijing 100190, China
E-mail: zhcheng@iphy.ac.cn
Prof. Z. Cheng
School of Physical Sciences
University of Chinese Academy of Sciences
Beijing 100049, China

DOI: 10.1002/adma.201706439

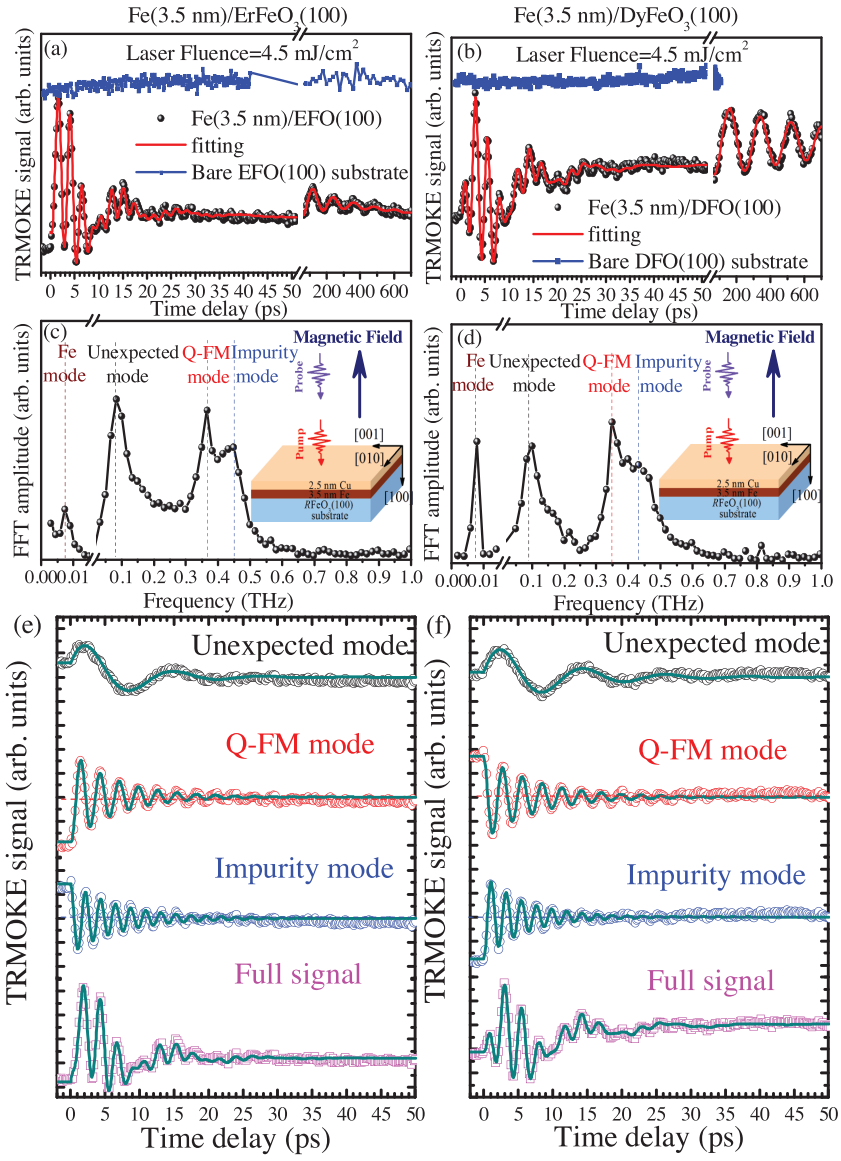

Figure 1. a,b) Room-temperature TRMOKE signals of Fe/EFO(100) (a) and Fe/DFO(100) (b) heterostructures with a laser fluence of 4.5 mJ cm^{-2}. c,d) Frequency component obtained by FFT method in the timescale of 0–50 ps. e,f) Individual contribution of the unexpected, Q-FM, and impurity modes to the full signal in Fe/EFO(100) (e) and Fe/DFO(100) (f) heterostructures. The dotted and solid curves are the experimental and fitting results, respectively. The field (2.5 kOe) was applied out-of-plane.

spin reorientation of a Co film coupled with $SmFeO_3$ has been achieved, no evident AFM spin dynamics has been observed in Co/$SmFeO_3$ heterostructures pumped by an ultrashort laser with a 800 nm wavelength,[18,19] which has been attributed to the large time resolution of the X-ray probe technique (≈15 ps) compared with the typical precession period (≈1–2 ps) of AFM spin dynamics.

In this communication, we present an all-optical pump-probe study on the spin dynamics of Fe/$RFeO_3$ (R = Er or Dy) heterostructures and demonstrate the multimode AFM spin dynamics in $RFeO_3$ in a broad temperature range (10–300 K). We found that with a capping Fe layer, not only the Q-FM and impurity modes, which are believed be excited only by all-optical pump-probe technique in the vicinity of spin-reorientation temperature and THz pulse field,[2–4,9] but also the Q-AFM and coherent phonon modes are triggered successfully by femtosecond lasers in the entire measured temperature range. Because ultrafast AFM spin dynamics is a key issue for exchange-biased spintronic devices, the significantly improved photoinduced excitation of multimode AFM spin dynamics achieved by simply capping a thin FM film can expand the application of AFM materials for spintronic devices.

Both EFO and DFO orthoferrites are Γ_4 phases at room temperature.[20] The temperature dependence of spin configuration for Fe/$RFeO_3$ heterostructures is discussed in detail in Figure S1 in the Supporting Information. The magneto-optical Kerr measurements suggest an obvious exchange bias effect in the Fe/$RFeO_3$ heterostructures (see Figure S2 in the Supporting Information). We have demonstrated that FM films are an AFM exchange coupled with $RFeO_3$.[21] We investigated the ultrafast AFM spin dynamics using the all-optical pump-probe technique. **Figure 1**a,b shows the room-temperature time-resolved magneto-optical Kerr effect (TRMOKE) signals of Fe/EFO(100) and Fe/DFO(100) heterostructures, respectively. For comparison, we also plotted the TRMOKE signals of bare EFO(100) and DFO(100) substrates. We applied the external magnetic field of 2.5 kOe along the *a* axis of $RFeO_3$ single crystals. Consistent with previous work, for temperatures far away from the phase transition temperature region, we did not observe any significant dynamic signals in the bare EFO and DFO single crystals using the all-optical method (see the blue dotted curves in Figure 1a,b).[2–4] Interestingly, after we covered the EFO and DFO substrates with a thin Fe film, we not only observed a slow spin precession mode of the Fe film in a time range of 50–700 ps (GHz range in frequency domain) but also observed fast precession modes in the time range of 0–50 ps (see the black dotted curves in Figure 1a,b). By analyzing the frequency spectrum with the faster Fourier transform (FFT) method, we obtained one mode with a resonant frequency of a few GHz (≈8 GHz for Fe/EFO and ≈6 GHz for Fe/DFO) and three obvious resonance modes among the THz region with frequencies of ≈0.08, ≈0.36, and ≈0.46 THz for both Fe/EFO(100) and Fe/DFO(100) (Figure 1c,d). Therefore, the damped dynamical signal (ΔM) in the timescale of 0–50 ps typically is fitted with three precession modes, and the relation can be expressed as follows

$$\Delta M(t) = \sum_{i=1,2,3} A_i \cos(2\pi f_i t + \varphi_i)\exp(-t/\tau_i) + B\exp(-t/\tau_0) + C \quad (1)$$

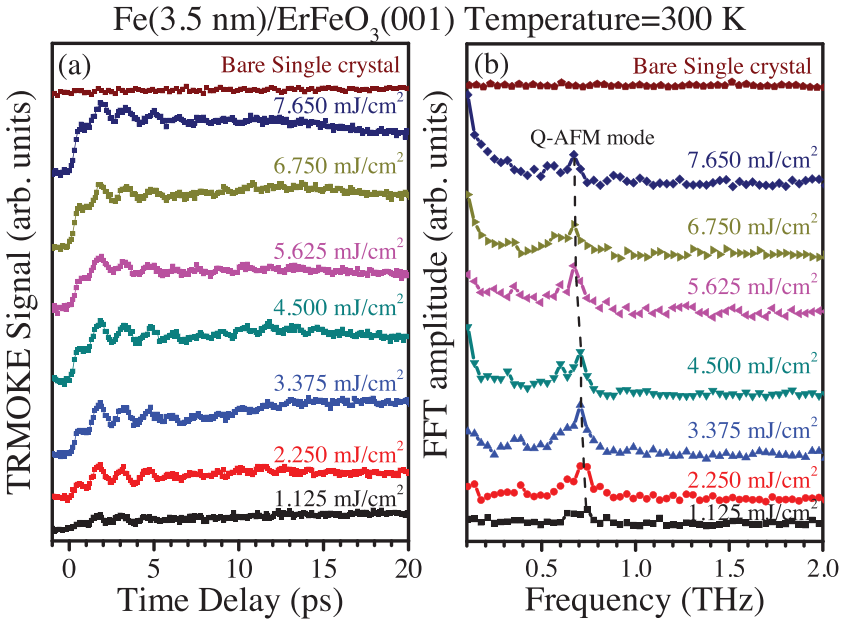

Figure 2. Multimode spin dynamics in Fe/EFO(001) heterostructure at 300 K: a) TRMOKE signals and b) corresponding FFT spectra. The dashed curves were plotted, guided by eyes. The field (2.5 kOe) was applied out-of-plane.

where the first three terms describe the magnetic precession of the three modes; the last two terms represent the background signal, including the dynamic signal of Fe film; A_i, f_i, t, φ_i, and τ_i (i = 1, 2, and 3) are the oscillatory amplitude, precession frequency, delay time, initial precession phase, and relaxation time, respectively, for three modes; B and C are both the background amplitude; and τ_o is the recovery time constant. According to Equation (1) without A_2 and A_3 terms, we also fitted the dynamic information for Fe film in the time range of 50–700 ps.

We obtained an excellent fitting based on Equation (1) (see the red curves in Figure 1a,b). One of the high-frequency modes with a frequency of ≈0.36 THz for Fe/EFO(100) and ≈0.35 THz for Fe/DFO(100) was very close to that of the Q-FM mode in $RFeO_3$, which was excited by a terahertz pulse field (0.377 THz for EFO and 0.3795 THz for DFO around room temperature).[11,22,23] Furthermore, upon decreasing the laser fluence, the values of frequency for this component were almost the same as previously reported values (see Figure S3 in the Supporting Information). Thus, we can assign this spectral component to the Q-FM mode of $RFeO_3$. We assigned the resonant peaks at ≈0.459 THz for EFO and ≈0.456 THz for DFO to the impurity modes of $RFeO_3$. The impurity modes were first reported in $TmFeO_3$ and EFO by Mikhaylovskiy et al. and were attributed to the occupation of the $^6A_1$ ground state of the Fe^{3+} ions in rare-earth positions.[8,9] The impurity mode in EFO and DFO, which has not been reported previously by the common all-optical method, has been observed only by THz emission spectroscopy. We assigned this mode to the impurity mode rather than the Q-AFM mode for two reasons. First, the resonant frequency is much smaller than the Q-AFM mode reported in previous work (0.673 THz for EFO and 0.510 THz for DFO around room temperature).[11,23] Second, by analyzing the individual contribution of these three modes to the full signal shown in Figure 1e,f, we found that the initial phase difference between this mode and the Q-FM mode was almost π, which is a typical characteristics for this impurity mode.[9,24]

In addition to the Q-FM and impurity modes, we observed an unexpected mode with a spectral component at ≈0.08 THz for EFO and DFO, which has never been reported for bare rare-earth orthoferrites. The frequencies of this unexpected mode were nearly independent of laser fluence (see Figure S3 in the Supporting Information). Furthermore, by changing the direction of the in-plane magnetization component, the unexpected modes also were insensitive to the magnetization orientation (see Figure S4 in the Supporting Information), which predicted its nonmagnetic behavior—that is, the phonon mode originated from the lattice oscillation.[25] Because of the polycrystalline nature of the Fe film, the coherent phonon mode is assigned only to the lattice oscillation of the EFO and DFO single-crystal substrates, which has not yet been demonstrated in bare rare-earth orthoferrites using the all-optical method. Recently, Raman phonons of A_{1g} + B_{1g} and B_{1g} symmetries with frequencies of 3.36 and 4.85 THz excited by a 20 THz mid-infrared pulse both have been reported in EFO.[12] The unpredicted phonon mode suggests that the coherent lattice oscillation in $RFeO_3$ may be more complicated than previously assumed.[26,27]

Figure 2a shows the representative dynamic signal of Fe/EFO(001) heterostructures at 300 K. We observed an evident oscillation with period at ≈1.4 ps. The corresponding FFT spectra with laser fluence varied from 1.125 to 7.65 mJ cm^{-2}, as shown in Figure 2b. All frequency spectra revealed a peak frequency at ≈0.7 THz, which is consistent with the Q-AFM mode of EFO (0.673 THz) obtained by THz time-domain spectroscopy and submillimeter backward-wave oscillator spectroscopy.[11,23] Recently, the crystal-field excitations of Er^{3+} at high frequency modes triggered by an ultrafast laser were obtained.[28] These excitation modes were determined only by the bandgap between different energy levels, which are different according to the frequency shift induced by the laser fluence of the observed mode (i.e., the peak frequency increases as fluence decreases, as shown in Figure 2b).

Figure 3a,b shows the temperature dependence of ultrafast spin dynamics of Fe/EFO(100) and Fe/EFO(001) heterostructures, respectively. In contrast to previous work related to AFM spin dynamics of bare $RFeO_3$ orthoferrites using the all-optical method, the ultrafast AFM spin dynamics of EFO in exchange-coupled heterostructures was triggered in the temperature range of 10–300 K. Similarly, the multimode spin dynamics of Fe/DFO heterostructures also could be probed in the temperature range of 10–300 K (see Figures S5 and S6 in the Supporting Information). Figure 3c shows the temperature dependence of multimode dynamic frequencies. The dynamic frequencies of

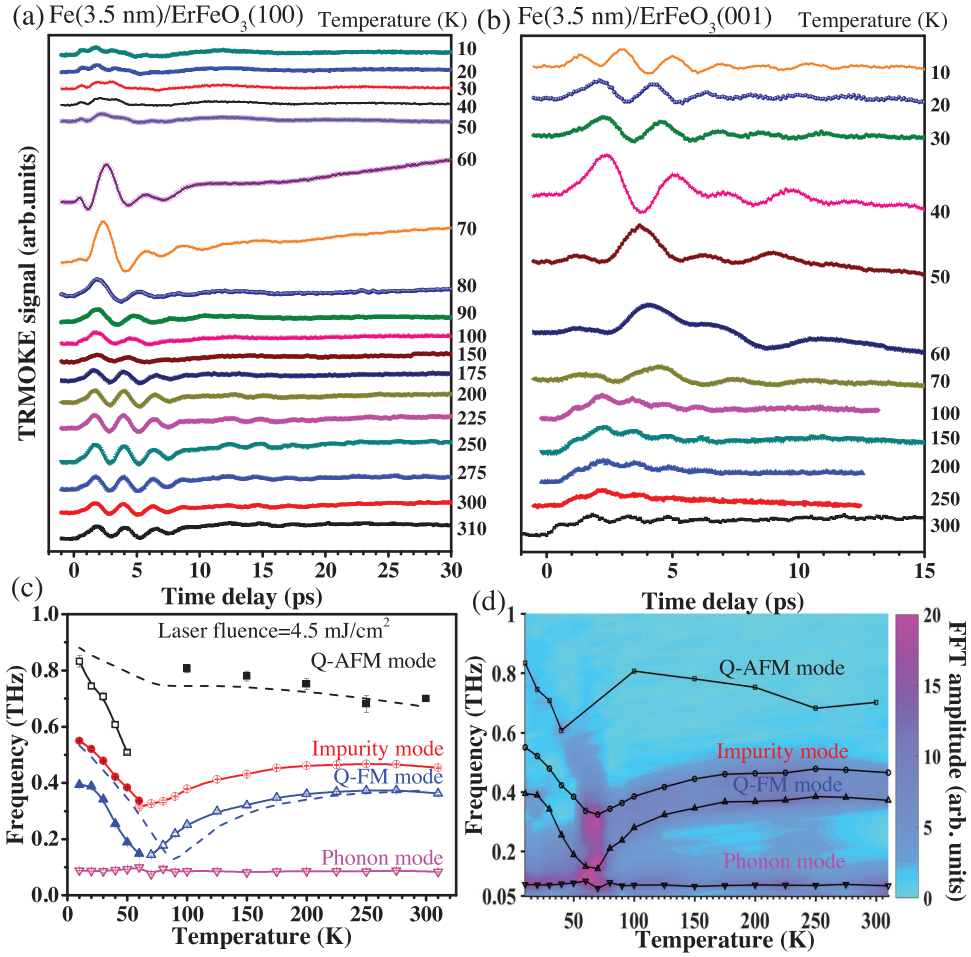

Figure 3. a,b) TRMOKE signal as a function of temperature in Fe/EFO(100) (a) and Fe/EFO(001) (b) heterostructures with a fixed laser fluence of 4.5 mJ cm^{-2}. c) Dynamic frequency of phonon, Q-FM, impurity, and Q-AFM modes as a function of temperature. The open and solid symbols are obtained from Fe/EFO(100) and Fe/EFO(001) heterostructures, respectively. d) The representative FFT amplitude as a function of temperature and frequency in Fe/EFO heterostructures. The field (2.5 kOe) was applied out-of-plane.

impurity and Q-FM modes decreased obviously in the vicinity of the spin-reorientation transition temperature, which is understood by the decrease of uniaxial magnetocrystalline anisotropy.[11] The temperature dependence of frequencies for the Q-FM and Q-AFM modes agreed well with that obtained by the THz time-domain spectroscopy method (see the dotted and dash curves in Figure 3c).[11] The highest dynamic mode was temperature dependent, which further confirmed that the crystal-field excitations of Er^{3+} was not responsible for this mode.[28] The resonant frequencies of Q-FM and Q-AFM modes were determined by the exchange interactions of Fe^{3+}-Fe^{3+} ions and Er^{3+}-Fe^{3+} ions. The slightly lower frequencies of the Q-AFM mode than the previously reported values possibly originated from the occupation of some Fe^{3+} ion on Er^{3+} sites, which decreased the exchange interactions of Fe^{3+}-Fe^{3+}ions and Er^{3+}-Fe^{3+} ions. In the vicinity of spin-reorientation transition of EFO orthoferrites, the dynamic signal exhibited the largest amplitude (Fe/EFO(100) at 60–70 K, Fe/EFO(001) at 40–60 K), which was similar to the experimental results obtained in single-crystal EFO orthoferrites using the common all-optical method.[2,3,7] Note that the temperature dependence of frequency for the impurity mode in a broad temperature range is rarely demonstrated elsewhere.[9] The dynamic frequency of the phonon mode exhibited temperature and magnetic field independence, confirming its nonmagnetic nature. Figure 3d shows the representative FFT amplitude of the TRMOKE signal in Fe/EFO(100) heterostructures as a function of temperature and frequency. The FFT peak values also revealed the largest amplitude in the temperature just below the spin-reorientation transition temperature region. Combing the spin dynamics of Fe/EFO(100) with Fe/EFO(001), we concluded that the Q-FM and impurity modes could be excited effectively by laser when compensated AFM and net FM spins lie out-of-plane and in-plane (see Figures S7 and S8 in the Supporting Information), respectively. Meanwhile, the Q-AFM mode can be probed only when AFM and net FM spins remained in-plane and out-of-plane (see Figures S7 and S8 in the Supporting Information), respectively. Additionally, the phonon mode could be obtained only in Fe/EFO(100) heterostructures regardless of the spin configuration of EFO orthoferrite.

Although the dramatic change of the ultrafast response in FM/nonmagnetic metallic heterostructures compared with the bare ferromagnets also has been reported,[29,30] the mechanism

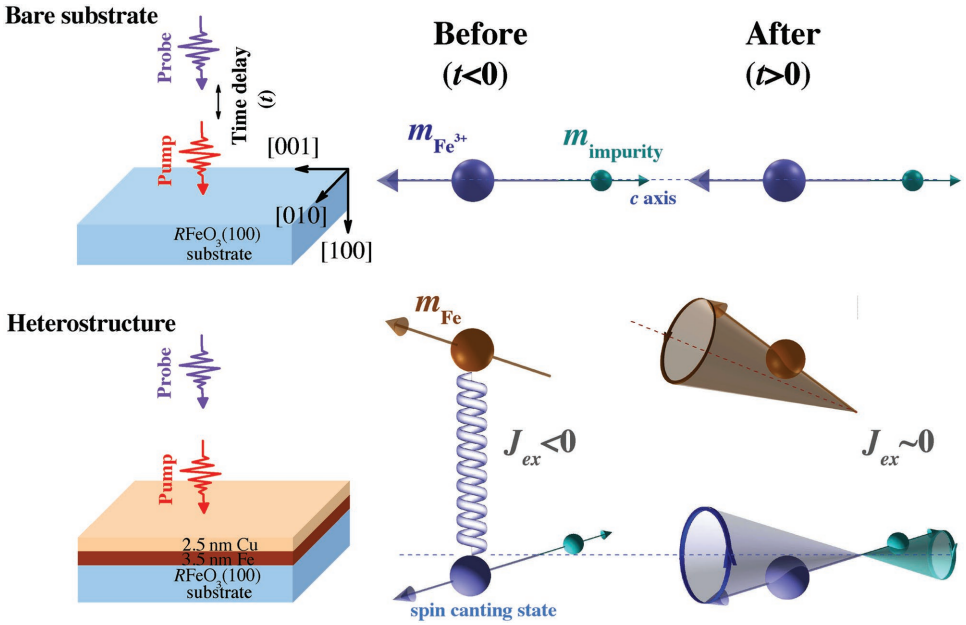

Figure 4. Schematic diagram of enhanced excitation of AFM spin dynamics in FM/$RFeO_3$(100) heterostructures with Γ_4 phase by optical modification of the interfacial exchange coupling.

of our observation could have been quite different. It is true that the activation of all modes of different symmetries (Q-FM and Q-AFM ones, impurity, and phonon modes) cannot be attributed to the same mechanism, but our work demonstrated that covering $RFeO_3$ with a thin FM film could trigger the multimode AFM spin dynamics. One reasonable explanation for the pronounced enhanced excitation of AFM spin dynamics in Fe/$RFeO_3$ heterostructures is the optical modification of the interfacial exchange coupling between the Fe film and neighboring Fe^{3+} ions, which is illustrated simply in **Figure 4**. Traditionally, the ultrafast laser heating-induced Q-FM mode is believed to be activated just below the spin-reorientation temperature region, where the magnetization orientation of rare-earth orthoferrites is sensitive to lattice temperature. Because of the limited optical absorption in $RFeO_3$ orthoferrites, the temperature increase is only about 20 K for the laser fluence of 10 mJ cm^{-2}.[3,9,18] On the basis of the calculation with the transfer matrix approach,[18,31,32] Figure S9b in the Supporting Information indicates that the Fe film can be heated strongly by the laser and, in this way, is demagnetized (see Figures S10 and S11 in the Supporting Information), whereas laser-induced heating and associated demagnetization do not play a significant role in the insulating orthoferrites. Therefore, for temperatures significantly higher or lower than the phase transition temperature region (87–96 K), the change of sublattice magnetization magnitude excited by laser heating in rare-earth orthoferrites is too small to be probed by the all-optical method. Conversely, although optical modification of magnetic anisotropies existed in EFO and DFO,[33] the net magnetization orientation of spin in rare-earth orthoferrites did not change when it remained along the initial equilibrium orientation at a temperature far from the spin-reorientation temperature. Therefore, the magnetization in rare-earth orthoferrites was barely disturbed by the pure laser heating-induced effect, resulting in no obvious dynamic signal.

In general, the thermal-induced magnetization dynamic process usually can be divided into three parts: an ultrafast demagnetization process, a magnetic recovery process, and a magnetic precession process.[2,34,35] The instant pronounced multimode precession without ultrafast demagnetization and thermal recovery processes (see the red and blue dotted curves shown in Figure 1e,f) further confirmed that the laser heating-induced lattice temperature increase was not crucial for the induced THz precession in $RFeO_3$ orthoferrites. In contrast, by covering the rare-earth orthoferrites with a thin FM film, the interfacial AFM spins did not remain strictly along the initial equilibrium axis, but rather they approached a new direction because of the strong AFM interfacial exchange interactions ($J_{ex} < 0$).[21] The AFM spins were able to rotate around the initial equilibrium axis because of the transient decrease of exchange coupling strength excited by a femtosecond laser, resulting in an enhanced precession magnitude compared with bare substrates. The amplitudes of static Kerr signals contributed to by the bare $RFeO_3$(100) were almost the same as the amplitudes in the Fe/$RFeO_3$ heterostructures (see Figure S12 in the Supporting Information), suggesting that the enhanced dynamic signals of AFM could be attributed to the enhanced precession of magnetization, rather than to the enhanced magneto-optical response of the $RFeO_3$ in the heterostructures. Optical modification of the interfacial exchange coupling, however, might have contributed to the enhanced excitation of the magnetic dynamic modes, but this failed to explain the enhanced excitation of the nonmagnetic mode (i.e., the phonon mode). Because the thermal gradient generated by a laser pulse in the heterostructure was present (see Figure S9 in the Supporting Information), the spin current of the FM film that resulted from the spin Seebeck effect could be considered to be another mechanism to excite the AFM spin dynamics of $RFeO_3$ orthoferrites.[31,36] Because of the large spin transfer length for the Cu

film (≈13 nm),[31] by inserting a Cu space layer with a thickness smaller than 13 nm, we expected AFM spin dynamics also to be excited by the spin-transfer torque effect. We did not obtain, however, any enhanced excitation of AFM spin dynamics by inserting a 2.5-nm Cu buffer layer to decouple the heterostructures (see Figure S13 in the Supporting Information), suggesting that the interfacial exchange coupling significantly enhanced the excitation of AFM spin dynamics by ultrafast laser. More theoretical and experimental work, including pump polarization dependence, photoinduced reduction of the interfacial exchange interaction, superposition of optical modification of the exchange interaction of orthoferrites, and spin transfer torque driven by the thermal gradient,[8,31] are required to further explore the mechanisms of ultrafast spin dynamics for $Fe/RFeO_3$ heterostructures.

In summary, we have studied the ultrafast photoinduced multimode spin dynamics of $Fe/RFeO_3$ heterostructures using TRMOKE. By covering $RFeO_3$ with a thin FM film, we have significantly improved the efficiency of multimode spin dynamics excited by ultrafast femtosecond laser pulses. By using the common all-optical pump-probe technique, the unexpected coherent phonon, Q-FM, impurity, and Q-AFM modes observed in $RFeO_3$ orthoferrites were all reported in a broad temperature range (10–300 K). We have proposed an accessible but effective method, that is, covering rare-earth orthoferrites with a thin FM film, to trigger the multimode spin dynamics of $RFeO_3$ orthoferrites in a wide temperature range using the all-optical pump-probe technique. Our work sheds light on ultrafast magnetization manipulation of AFM in spin-valve devices.

Experimental Section

Spin Dynamic Measurements: Spin dynamics was investigated using an all-optical TRMOKE setup. Also, a Ti:sapphire oscillator (Femtolaser XL-100, Femtolasers Produktions GmbH, Vienna, Austria) was used with a repetition rate of 5.2 MHz, duration of 55 fs, and wavelength of 780 nm as the pump laser, which was linearly polarized perpendicular to the projection direction. The 780 nm wavelength laser doubled the frequency by a nonlinear optical crystal BaB_2O_4 with a thickness of 200 µm, and the probe laser was linearly polarized along the projection direction. The pump and probe beams were focused onto the sample with spot diameters of 10 and 5 µm via a 20× objective at normal incidence, respectively. For variable temperature measurements, the samples were put in a cryostat cooled by liquid helium. The sample temperature was controlled precisely using a Lake Shore Cryotronics (Westerville, OH, USA) model 340 temperature controller with a stability of <0.01 K h^{-1}. The thermometer was not directly attached to the sample, and a small additional temperature (10–20 K) gradient between the sample and the thermometer was present. The dynamical Kerr signal was sensitive only to the changes in the out-of-plane magnetization component.

Supporting Information

Supporting Information is available from the Wiley Online Library or from the author.

Acknowledgements

This work was supported by the National Key Research Program of China (Grant Nos. 2016YFA0300701, 2015CB921403, and 2017YFB0702702), the National Natural Sciences Foundation of China (Grant Nos. 91622126, 51427801, and 51671212), and the Key Research Program of Frontier Sciences, CAS (Grant Nos. QYZDJ-SSW-JSC023, KJZD-SW-M01, and ZDYZ2012-2).

Conflict of Interest

The authors declare no conflict of interest.

Keywords

all-optical pump probes, antiferromagnetic-based spintronics, exchange-coupled heterostructures, multimode antiferromagnetic spin dynamics

Received: November 5, 2017
Revised: April 15, 2018
Published online:

[1] T. Jungwirth, X. Marti, P. Wadley, J. Wunderlich, *Nat. Nanotechnol.* **2016**, *11*, 231.
[2] A. V. Kimel, A. Kirilyuk, A. Tsvetkov, R. V. Pisarev, T. Rasing, *Nature* **2004**, *429*, 850.
[3] J. A. de Jong, A. V. Kimel, R. V. Pisarev, A. Kirilyuk, T. Rasing, *Phys. Rev. B* **2011**, *84*, 104421.
[4] A. V. Kimel, C. D. Stanciu, P. A. Usachev, R. V. Pisarev, V. N. Gridnev, A. Kirilyuk, T. Rasing, *Phys. Rev. B* **2006**, *74*, 060403(R).
[5] A. V. Kimel, A. Kirilyuk, P. A. Usachev, R. V. Pisarev, A. M. Balbashov, T. Rasing, *Nature* **2005**, *435*, 655.
[6] R. Iida, T. Satoh, T. Shimura, K. Kuroda, B. A. Ivanov, Y. Tokunaga, Y. Tokura, *Phys. Rev. B* **2011**, *84*, 064402.
[7] A. V. Kimel, B. A. Ivanov, R. V. Pisarev, P. A. Usachev, A. Kirilyuk, T. Rasing, *Nat. Phys.* **2009**, *5*, 727.
[8] R. V. Mikhaylovskiy, E. Hendry, A. Secchi, J. H. Mentink, M. Eckstein, A. Wu, R. V. Pisarev, V. V. Kruglyak, M. I. Katsnelson, T. Rasing, A. V. Kimel, *Nat. Commun.* **2015**, *6*, 8190.
[9] R. V. Mikhaylovskiy, E. Hendry, V. V. Kruglyak, R. V. Pisarev, T. Rasing, A. V. Kimel, *Phys. Rev. B* **2014**, *90*, 184405.
[10] S. Baierl, M. Hohenleutner, T. Kampfrath, A. Zvezdin, A. Kimel, R. Huber, R. Mikhaylovskiy, *Nat. Photonics* **2016**, *10*, 715.
[11] K. Yamaguchi, T. Kurihara, Y. Minami, M. Nakajima, T. Suemoto, *Phys. Rev. Lett.* **2013**, *110*, 137204.
[12] T. F. Nova, A. Cartella, A. Cantaluppi, M. Forst, D. Bossini, R. V. Mikhaylovskiy, A. V. Kimel, R. Merlin, A. Cavalleri, *Nat. Phys.* **2017**, *13*, 132.
[13] G. Ju, A. Nurmikko, R. Farrow, R. Marks, M. Carey, B. Gurney, *Phys. Rev. B* **1998**, *58*, R11857.
[14] G. Ju, A. Nurmikko, R. Farrow, R. Marks, M. Carey, B. Gurney, *Phys. Rev. Lett.* **1999**, *82*, 3705.
[15] F. Dalla Longa, J. T. Kohlhepp, W. J. M. de Jonge, B. Koopmans, *Phys. Rev. B* **2010**, *81*, 094435.
[16] F. Hellman, A. Hoffmann, Y. Tserkovnyak, G. S. D. Beach, E. E. Fullerton, C. Leighton, A. H. MacDonald, D. C. Ralph, D. A. Arena, H. A. Dürr, P. Fischer, J. Grollier, J. P. Heremans, T. Jungwirth, A. V. Kimel, B. Koopmans, I. N. Krivorotov, S. J. May, A. K. Petford-Long, J. M. Rondinelli, N. Samarth, I. K. Schuller, A. N. Slavin, M. D. Stiles, O. Tchernyshyov, A. Thiaville, B. L. Zink, *Rev. Mod. Phys.* **2017**, *89*, 025006.
[17] X. Ma, F. Fang, Q. Li, J. Zhu, Y. Yang, Y. Z. Wu, H. B. Zhao, G. Lupke, *Nat. Commun.* **2015**, *6*, 8800.
[18] L. Le Guyader, A. Kleibert, F. Nolting, L. Joly, P. M. Derlet, R. V. Pisarev, A. Kirilyuk, T. Rasing, A. V. Kimel, *Phys. Rev. B* **2013**, *87*, 054437.

[19] L. Joly, F. Nolting, A. V. Kimel, A. Kirilyuk, R. V. Pisarev, T. Rasing, *J. Phys.: Condens. Matter* **2009**, *21*, 446004.
[20] R. L. White, *J. Appl. Phys.* **1969**, *40*, 1061.
[21] J. Tang, Y.-J. Ke, W. He, X.-Q. Zhang, Y.-S. Zhang, W. Zhang, Y. Li, S. S. Ahmad, Z.-H. Cheng, *J. Phys. D: Appl. Phys.* **2017**, *50*, 205001.
[22] A. H. M. Reid, T. Rasing, R. V. Pisarev, H. A. Dürr, M. C. Hoffmann, *Appl. Phys. Lett.* **2015**, *106*, 082403.
[23] G. V. Kozlov, S. P. Lebedev, A. A. Mukhin, A. S. Prokhorov, I. V. Fedorov, A. M. Balbashov, I. Y. Parsegov, *IEEE Trans. Magn.* **1993**, *29*, 3443.
[24] A. A. Mukhin, A. N. Lobanov, M. Goiran, J. Leotin, A. A. Volkov, *J. Magn. Reson.* **2008**, *195*, 60.
[25] A. M. Kalashnikova, A. V. Kimel, R. V. Pisarev, V. N. Gridnev, P. A. Usachev, A. Kirilyuk, T. Rasing, *Phys. Rev. B* **2008**, *78*, 104301.
[26] D. M. Juraschek, M. Fechner, N. A. Spaldin, *Phys. Rev. Lett.* **2017**, *118*, 054101.
[27] V. D. Buchel'nikov, N. K. Dan'shin, L. T. Tsymbal, V. G. Shavrov, *Phys.-Usp.* **1996**, *39*, 547.
[28] R. V. Mikhaylovskiy, T. J. Huisman, R. V. Pisarev, T. Rasing, A. V. Kimel, *Phys. Rev. Lett.* **2017**, *118*, 017205.
[29] T. Kampfrath, M. Battiato, P. Maldonado, G. Eilers, J. Nötzold, S. Mährlein, V. Zbarsky, F. Freimuth, Y. Mokrousov, S. Blügel, *Nat. Nanotechnol.* **2013**, *8*, 256.
[30] T. J. Huisman, R. V. Mikhaylovskiy, J. D. Costa, F. Freimuth, E. Paz, J. Ventura, P. P. Freitas, S. Blugel, Y. Mokrousov, T. Rasing, A. V. Kimel, *Nat. Nanotechnol.* **2016**, *11*, 455.
[31] A. J. Schellekens, K. C. Kuiper, R. R. de Wit, B. Koopmans, *Nat. Commun.* **2014**, *5*, 4333.
[32] K. Ohta, H. Ishida, *Appl. Opt.* **1990**, *29*, 1952.
[33] K. Yamaguchi, T. Kurihara, H. Watanabe, M. Nakajima, T. Suemoto, *Phys. Rev. B* **2015**, *92*, 064404.
[34] M. van Kampen, C. Jozsa, J. T. Kohlhepp, P. LeClair, L. Lagae, W. J. M. de Jonge, B. Koopmans, *Phys. Rev. Lett.* **2002**, *88*, 227201.
[35] Y. Xu, M. Deb, G. Malinowski, M. Hehn, W. Zhao, S. Mangin, *Adv. Mater.* **2017**, *29*, 1703474.
[36] K. Uchida, S. Takahashi, K. Harii, J. Ieda, W. Koshibae, K. Ando, S. Maekawa, E. Saitoh, *Nature* **2008**, *455*, 778.